NASA TECHNICAL MEMORANDUM

NASA TM X-2348

NASA TM X-2348

INTERFACE STABILITY DURING LIQUID INFLOW TO PARTIALLY FULL, HEMISPHERICAL ENDED CYLINDERS DURING WEIGHTLESSNESS

by Eugene P. Symons and John V. Staskus

Lewis Research Center

Cleveland, Ohio 44135

NATIONAL AERONAUTICS AND SPACE ADMINISTRATION • WASHINGTON, D. C. • AUGUST 1971

1. Report No.	2. Government Accession No.	3. Recipient's Catalog No.
NASA TM X-2348		

4. Title and Subtitle	5. Report Date
INTERFACE STABILITY DURING LIQUID INFLOW TO PARTIALLY FULL, HEMISPHERICAL ENDED CYLINDERS DURING WEIGHTLESSNESS	August 1971
	6. Performing Organization Code

7. Author(s)	8. Performing Organization Report No.
Eugene P. Symons and John V. Staskus	E-6346
	10. Work Unit No. 124-08

9. Performing Organization Name and Address	11. Contract or Grant No.
Lewis Research Center National Aeronautics and Space Administration Cleveland, Ohio 44135	

12. Sponsoring Agency Name and Address	13. Type of Report and Period Covered
National Aeronautics and Space Administration Washington, D.C. 20546	Technical Memorandum
	14. Sponsoring Agency Code

15. Supplementary Notes

16. Abstract

The stability of the liquid-vapor interface during liquid inflow to a partially full hemispherical ended cylinder during weightlessness was studied. The investigation was limited to one tank radius (2 cm), one inlet line radius (0.2 cm), and three test liquids (ethanol, carbon tetrachloride, and trichlorotrifluoroethane). A stable region and an unstable region of interface behavior were noted. The velocity which delineated between the two regimes was termed the critical inflow velocity. Results indicate that the critical inflow velocity increases with increasing initial liquid depth and further indicate that this increase is more pronounced when the initial velocity profile of the incoming liquid jet is uniform rather than partially parabolic.

17. Key Words (Suggested by Author(s))	18. Distribution Statement
Weightlessness Propellant transfer	Unclassified - unlimited

19. Security Classif. (of this report)	20. Security Classif. (of this page)	21. No. of Pages	22. Price*
Unclassified	Unclassified	27	$3.00

*For sale by the National Technical Information Service, Springfield, Virginia 22151

INTERFACE STABILITY DURING LIQUID INFLOW TO PARTIALLY FULL, HEMISPHERICAL ENDED CYLINDERS DURING WEIGHTLESSNESS

by Eugene P. Symons and John V. Staskus

Lewis Research Center

SUMMARY

The stability of the liquid-vapor interface during liquid inflow to a partially full hemispherical ended cylinder during weightlessness was studied. The investigation was limited to one tank radius (2 cm) one inlet line radius (0. 2 cm), and three test liquids (ethanol, carbon tetrachloride, and trichlorotrifluoroethane). A stable region and an unstable region of interface behavior were noted. The velocity which delineated between the two regimes was termed the critical inflow velocity. Results indicate that the critical inflow velocity increases with increasing initial liquid depth and further indicate that this increase is more pronounced when the initial velocity profile of the incoming liquid jet is uniform rather than partially parabolic.

INTRODUCTION

In-orbit propellant transfer (refueling) and the transfer of liquids between containers as in regenerative life support systems will be required for future space missions. A knowledge of both the outflow characteristics from a storage tank and the subsequent fluid behavior during filling of the receiver tank under weightlessness is required for the design of such transfer systems. The Lewis Research Center is presently conducting programs to investigate these phenomena.

In previous studies (refs. 1 and 2), the author investigated liquid-vapor interface behavior during the filling of an initially empty hemispherical ended cylinder in a weightless environment. In those studies, both a stable liquid-vapor interface characterized by relatively little interface distortion and an unstable interface characterized by a large degree of interface distortion were observed. It was determined that the stability of the interface could be delineated by a Weber number based on inlet line radius and average inflow velocity.

A recently completed extension of those studies (ref. 3) consisted of an investigation of the behavior of the liquid-vapor interface during liquid inflow to a hemispherical ended cylinder partially full of liquid at the initiation of inflow. Once again, the study was conducted in a weightless environment and both a stable and an unstable liquid-vapor interface were observed. It was determined that the critical inflow velocity (the velocity above which the interface becomes unstable) remained constant until a certain initial depth of liquid above the inlet line was obtained. At larger initial depths, the critical inflow velocity was found to increase with increasing initial liquid depth.

This report presents the results of an investigation of the interface stability during liquid inflow to partially full hemispherical ended cylinders in which the inlet line geometry is modified so as to provide a uniform velocity profile to the incoming liquid jet in contrast to the partially parabolic velocity profile of the incoming jet in reference 3. Results are presented in photographic and graph form and are compared with the results of reference 3. The study was conducted in the Lewis Research Center 2.2-Second Zero-Gravity Facility and was limited to one tank radius (2 cm), one inlet line radius (0.2 cm), and three test liquids (ethanol, carbon tetrachloride, and trichlorotrifluoroethane).

SYMBOLS

D_i	inlet line diameter, cm
H_i	height of zero-gravity liquid-vapor interface above inlet line, cm
h	height above inlet, cm
R_i	inlet line radius, cm
R_j	jet radius, cm
Re	jet Reynolds number, $\rho V_{i,av} D_i / \mu$
r	radial distance from tank axis, cm
$V_{(h,r)}$	axial component of liquid velocity at distance h above inlet and r from axis, cm/sec
$V_{i,av}$	average inflow velocity, cm/sec
$V_{i,av,cr}$	critical average inflow velocity, cm/sec
We	Weber number
β	specific surface tension, σ/ρ, cm^3/sec^2
μ	viscosity, g/(cm)(sec)

ρ density, g/cm^3

σ surface tension, N/cm; dynes/cm

APPARATUS AND PROCEDURE

The investigation was conducted in the Lewis Research Center 2.2-Second Zero-Gravity Facility. A complete description of the facility, the experiment package, and the test procedure can be found in the appendix.

The experiment tank used in this investigation (see fig. 1) was a 4-centimeter-inside-diameter hemispherical-ended cylinder machined from cast acrylic rod and polished to optical clarity. The 30° convergent configuration of the 0.4-centimeter-diameter inlet was selected to provide a nearly uniform velocity profile of the incoming liquid jet at the nozzle exit. The tank was vented to the atmosphere through a port located along the longitudinal axis of the tank and directly opposite the inlet line.

Three liquids (ethanol, carbon tetrachloride, and trichlorotrifluoroethane) were employed. Properties pertinent to this study are presented in table I. All liquids had an essentially 0° static contact angle with the tank material in order to duplicate the contact angle of most spacecraft liquids on tank materials. A small amount of dye was added to the liquids in order to improve the photography. Previous studies had determined that the addition of the dye has no measurable effect on the fluid properties.

DATA REDUCTION

All data were recorded photographically with a high-speed camera. Volumetric flow out of a graduated cylinder and into the experiment tank was directly determined by taking readings of the liquid level at small time increments (read on the digital clock). From these readings, the average inflow velocity was calculated and found to remain essentially constant in a given test.

RESULTS AND DISCUSSION

Description of Interface Behavior

A stable region and an unstable region of interface behavior were noted. The stable region was characterized by the formation of a geyser which either remained at the same height or decreased in height with respect to the lowest point on the liquid-vapor

interface during inflow and, thus, the incoming liquid was successfully being retained at the inlet end of the tank. A photographic sequence illustrating this type of interface behavior is shown in figure 2. The first photograph in each sequence shows the interface as it appears in normal gravity prior to the test; the second shows the typical zero-gravity interface configuration; and the final two show the interface behavior during the inflow process. Note that the interface has been somewhat flattened by the incoming liquid jet.

The unstable region (fig. 3) was characterized by the formation of a geyser which continued to grow in height with respect to the lowest point on the liquid-vapor interface. In most cases, the liquid geyser persisted as a continuous column of liquid; however, in some tests, the geyser necked down and broke up into one or more liquid droplets which continued toward the vent end of the tank. In this region, only a portion of the incoming liquid collected over the inlet line, and continuation of inflow would have resulted in liquid impinging on the tank vent. The general behavior of the liquid-vapor interface for incoming jets having a partially parabolic velocity profile (ref. 3) was very similar to that observed in the present study.

Effect of Initial Velocity Profile on Critical Inflow Velocity

Figure 4 illustrates the effect of initial velocity profile on critical inflow velocity. The individual points show the dependence of critical inflow velocity on initial liquid depth above the inlet for jets having an initially uniform velocity profile. The solid line was obtained from reference 3 data and is for jets having a partially parabolic profile. The comparison is made for the same test liquid, same tank radius, and same inlet line radius. Note that, for any given value of dimensionless initial liquid depth, the critical inflow velocity (average velocity for partially parabolic profile) is greater for the data in which the initial velocity profile was uniform. This figure is only drawn for comparison purposes and, as such, no best-fit line was drawn through the data; however, it does serve the purpose of illustrating that larger values of critical inflow velocity are obtained by designing an inlet line which provides the entering liquid jet with a uniform velocity profile.

Weber Number Criterion

Previous studies by the author (refs. 1 to 3) have resulted in development of various forms of the Weber number which should predict liquid-vapor interface stability during inflow to hemispherical ended tanks. By definition, the Weber number (ratio of momentum flux to suface-tension force) is

$$We = \frac{\int_0^{R_j} \rho \left[2\pi r \, dr \, V_{(h, r)}\right] V_{(h, r)}}{2\pi R_j \sigma} \tag{1}$$

Because of conservation of momentum, we may perform the integration at the inlet with the result that

$$We = \frac{\int_0^{R_i} \rho \left[2\pi r \, dr \, V_{(0, r)}\right] V_{(0, r)}}{2\pi R_j \sigma}$$

For a parabolic jet velocity profile

$$V_{(0, r)} = V_{(0, 0)} \left[1 - \left(\frac{r}{R_i}\right)^2\right]$$

The resulting Weber number is

$$We = \frac{V_{(0, 0)}^2 R_i^2}{6\beta R_j}$$

It can be shown that the centerline velocity $V_{(0, 0)}$ is twice the average velocity, so that the final form of the Weber number is

$$We = \frac{2}{3} \frac{V_{i, av}^2 R_i^2}{\beta R_j} \tag{2}$$

Similarly, for a uniform jet velocity profile

$$We = \frac{\rho \pi R_i^2 V_{(0, 0)}^2}{2\pi R_j \sigma} = \frac{1}{2} \frac{V_{i, av}^2 R_i^2}{\beta R_j} \tag{3}$$

Equations (2) and (3) give the Weber numbers for tanks containing some liquid with the interface at a distance h from the inlet. For initially empty tanks, $R_j = R_i$, and the Weber numbers become

$$We = \frac{2}{3} \frac{V_{i,av}^2 R_i}{\beta} \tag{4}$$

for a parabolic profile, and

$$We = \frac{1}{2} \frac{V_{i,av}^2 R_i}{\beta} \tag{5}$$

for a uniform profile. The critical Weber numbers are obtained when the critical inflow velocities are substituted in the formulas. In both past and present inflow studies, no attempt was made to determine the inlet velocity profile of the incoming liquid jet. However, in previous studies, the Weber number developed for the uniform inlet velocity profile was used to correlate the data. Thus, the critical Weber number determined in reference 1 for empty tanks was 1.3. If the Weber number developed for a parabolic inlet velocity profile had been used, the resulting value of the critical Weber number would have been 1.7. In reality, the inlet velocity profile of the jet in that study was neither uniform nor fully developed parabolic, but between the two extremes. The constant preceding the variable terms in equations (2) and (3) should be expected to have a value between the 1/2 for a uniform profile and the 2/3 for a fully developed parabolic profile. If a number midway between the two constants is selected, say 7/12, the actual magnitude of the critical Weber number as determined from the data would be 1.5. This number may be more representative of earlier data and might be expected to be the value of the critical Weber number for any velocity profile shape.

For the form of the critical Weber number developed for partially full tanks, a knowledge of the spreading characteristics of the incoming jet as well as the initial profile shape is also required. An experimental investigation (ref. 4) has shown that, in a gaseous environment, gaseous jets having a uniform velocity profile and moderate to high Reynolds numbers ($Re > 1500$), should be expected to spread to about 6° to 8° on each side of the jet centerline for a distance of 6.2 inlet line diameters and then at about 10° to 12° on each side of the jet centerline for distances greater than 6.2 inlet line diameters. Another study (ref. 5) for jets (gas into gas) having a parabolic inlet velocity and Reynolds numbers below about 1850 found that the jets spread at an angle of about 2° to 3° on either side of the jet centerline.

A plot of the present data using the critical Weber number developed for a uniform profile jet entering an initially empty tank, equation (5), was made (fig. 5) with the assumption that a liquid into liquid jet spreads similarly to a gas into gas jet. This Weber number differs from the critical Weber number developed for a uniform profile jet entering a partially full tank, equation (3), only by the radius ratio R_i/R_j. A linear increase in the empty tank Weber number would indicate a linear decrease in R_i/R_j (i.e., a constant angle of jet spreading). From the nominal angles of spread determined in reference 4 (7^o and 11^o), it is possible to determine the parameter R_i/R_j as a function of H_i/D_i. When the critical Weber number (1.5) is divided by the values of R_i/R_j thus determined, it is possible to generate the solid line shown in figure 5(a). Note that this line does delineate between the region of stable interface behavior and the region of unstable interface behavior. This agreement lends support to the use of the following expression to delineate between stable and unstable interface behavior:

$$We_{cr} = 1.5 = \frac{V_{i,av,cr}^2 R_i}{2\beta}\left(\frac{R_i}{R_j}\right) \tag{6}$$

where

$$R_j = R_i + H_i \tan 7^o \qquad H_i \leq 12.4\, R_i$$

$$R_j = R_i\left[1 + 12.4(\tan 7^o - \tan 11^o)\right] + H_i \tan 11^o \qquad H_i > 12.4\, R_i$$

These expressions can be approximated by

$$R_j = R_i + 0.12\, H_i \qquad H_i \leq 12.4\, R_i$$

$$R_j = 0.11\, R_i + 0.19\, H_i \qquad H_i > 12.4\, R_i$$

The foregoing is predicated on the assumption that the jet Reynolds number is greater than 1500 and the velocity profile is uniform.

The other test liquid used in the present investigation was ethanol. While the initial velocity profile shape can be assumed to be uniform, the lower Reynolds numbers in these tests ($500 < Re < 750$) may have resulted in a smaller angle of spread. If the data points for ethanol are plotted in a manner similar to that for carbon tetrachloride and trichlorotrifluoroethane, the curve shown in figure 5(b) is obtained. This curve also shows that two regions of spreading occur. The first region extends for a distance of

8 inlet diameters and its associated spreading angle is 2°. The angle of spread for the second region is 4°. These smaller angles are not to be wholly unexpected since Rouse (ref. 6) states that, if the Reynolds number is low, the rate of expansion of the jet will be smaller than that obtained at high Reynolds numbers. Sufficient data are not presently available to define adequately the functional relation between jet spreading and Reynolds number for Reynolds numbers less than about 1500 and uniform jet velocity profiles. For this reason, it is not recommended that equation (6) (with R_j developed from fig. 5(b)) be used to delineate between stable and unstable interface behavior in this region.

It should be emphasized that, although the curves presented in figure 5 do tend to support the validity of the critical Weber number criterion, the data obtained were not sufficient to prove this contention conclusively. To do so, more tests would have to be conducted in which inlet line sizes, tank sizes, and test liquids were varied. However, it is the opinion of the authors that the curve presented in figure 5(a) should be valid in predicting critical inflow velocity as a function of dimensionless initial liquid depth provided the initial velocity profile of the incoming liquid jet is uniform and the Reynolds number (based on inlet diameter) exceeds 1500. In most applications the Reynolds number should exceed this value and a judicious design of the inlet line could provide the uniform velocity profile.

SUMMARY OF RESULTS

An experimental investigation was conducted to determine the stability of the liquid-vapor interface during liquid inflow to a partially full, hemispherical ended cylindrical tank in a weightless environment. The shape of the inlet line was configured so as to provide a uniform velocity profile to the incoming liquid jet. The behavior of the liquid-vapor interface was observed over a range of initial liquid depths at various inflow velocities for one inlet radius (0.2 cm), one tank radius (2 cm), and three test liquids (ethanol, carbon tetrachloride, and trichlorotrifluoroethane). The Reynolds numbers (based on inlet line diameter and average inflow velocity) varied from about 500 to 750 for ethanol and from about 1400 to 2500 for carbon tetrachloride and trichlorotrifluoroethane. The following results were obtained:

1. A stable region and an unstable region of interface behavior were noted. In the stable region, liquid collected over the inlet line during inflow, and while a geyser formed, it either remained at a constant height or decreased in height with respect to the lowest point on the liquid-vapor interface. In the unstable region, the incoming liquid formed a geyser which moved toward the tank vent and, hence, relatively little liquid was collected over the inlet line.

2. The critical inflow velocity continually increased with increasing initial liquid depth. This contrasts with the results reported in NASA TM X-1934 for similar tanks in which the initial jet velocity profile was partially parabolic. In those tests, the critical inflow velocity remained constant for liquid depths below a value which was dependent on the type of liquid used, while for greater liquid depths, the critical inflow velocity increased slightly with increasing depth.

3. The rate of the increase in critical inflow velocity with increasing initial liquid depth is greater for inlets designed to provide an initially uniform velocity profile of the incoming liquid jet than it is for incoming jets having a partially parabolic profile at nozzle exit.

4. A critical Weber number based on average inflow velocity, inlet line radius and radius of the incoming liquid jet as it reaches the liquid-vapor surface may be useful in predicting interface stability for inflow to partially full tanks.

Lewis Research Center,
National Aeronautics and Space Administration,
Cleveland, Ohio, May 28, 1971,
124-08.

APPENDIX - APPARATUS AND PROCEDURE

Test Facility

The experimental data for this study were obtained in the Lewis Research Center 2.2-Second Zero-Gravity Facility. A schematic diagram of this facility is shown in figure 6. The facility consists of a building 6.4 meters (21 ft) square by 30.5 meters (100 ft) tall. Contained within the building is a drop area 27 meters (89 ft) long with a cross section of 1.5 by 2.75 meters (5 by 9 ft).

The service building has, as its major elements, a shop and service area, a calibration room, and a controlled environment room. Those components of the experiment which require special handling are prepared in the controlled environment room of the facility. This air-conditioned and filtered room (shown in fig. 7) contains an ultrasonic cleaning system and the laboratory equipment necessary for handling test liquids.

Mode of operation. - A 2.2-second period of weightlessness is obtained by allowing the experiment package to free fall from the top of the drop area. In order to minimize drag on the experiment package, it is enclosed in a drag shield, designed with a high ratio of weight to frontal area and a low drag coefficient. The relative motion of the experiment package with respect to the drag shield during a test is shown in figure 8. Throughout the test the experiment package and drag shield fall freely and independently of each other; that is, no guide wires, electrical lines, etc., are connected to either. Therefore, the only force acting on the freely falling experiment package is the air drag associated with the relative motion of the package within the enclosure of the drag shield. This air drag results in an equivalent gravitational acceleration acting on the experiment, which is estimated to be below 10^{-5} g.

Release system. - The experiment package, installed within the drag shield, is suspended at the top of the drop area by a highly stressed music wire which is attached to the release system. This release system consists of a double-acting air cylinder with a hard steel knife attached to the piston. Pressurization of the air cylinder drives the knife edge against the wire which is backed by an anvil. The resulting notch causes the wire to fail and smoothly release the experiment. No measurable disturbances are imparted to the package by this release procedure.

Recovery system. - After the experiment package and drag shield have traversed the total length of the drop area and have been decelerated in a 2.2-meter (7-ft) deep container filled with sand, they are recovered. The deceleration rate (averaging 15 g's) is controlled by selectively varying the tips of the deceleration spikes mounted on the bottom of the drag shield (fig. 6). At the time of impact of the drag shield in the decelerator container, the experiment package has traversed the vertical distance within the drag shield (compare figs. 8(a) and (c)).

Experiment Package

The experiment package shown in figure 9 is a self-contained unit consisting of an experiment tank, a pumping system, a photographic system, a digital clock, and an electrical system to operate the various components. Indirect illumination of the experiment tank provides sufficient light so that the behavior of the liquid-vapor interface can be recorded with a high-speed 16-millimeter motion-picture camera. An air reservoir, a graduated cylinder, a metering valve, and a solenoid valve make up the pumping system shown in figure 10. The volume of the air reservoir is approximately 30 times greater than the largest volume of liquid removed from the graduated cylinder during the transfer operation so that no significant pressure decrease occurs. Time during weightlessness is observed by reading a digital clock having an accuracy of ±0.01 second. The clock and all other electrical components are operated through a control box and receive their power from rechargeable nickel-cadmium cells.

Test Procedure

Prior to assembling the flow components, the tank and all the flow lines were first cleaned in an ultrasonic cleaner to assure that the properties of the test liquids would not be affected by contaminants. The parts were then rinsed with distilled water and dried in a warm air dryer. All parts were assembled and mounted in the package.

The flow lines were filled with liquid and activated several times to remove any air that may have been trapped in the lines. The system was checked for leaks; a normal-gravity calibration test was conducted to set the desired flow rate; and the timer was set at a predetermined time increment. This set the time when the solenoid valve would open and initiate inflow of liquid to the experiment tank. The timer setting was chosen so as to start inflow when the liquid-vapor interface had reached the low point in its first pass through the zero-gravity equilibrium configuration.

Since this time, which allowed for interface formation, is a function of tank size as well as fluid properties (ref. 7), it was a limiting factor in determining the maximum tank size that could be used in the investigation. If the time required for the interface to reach the low point in its first pass through equilibrium was too large, the remaining time in weightlessness would not be long enough to determine adequately the stability of the interface.

The desired quantity of test liquid was then placed in the graduated cylinder and the experiment tank, and the required pressure was supplied to the air reservoir. The camera was then loaded, and the experiment package was balanced about its horizontal axes and positioned in the prebalanced drag shield. The wire support was then attached to the experiment package through an access hole in the drag shield (see fig. 8). Prop-

erly sized spike tips were installed on the shield. Then the drag shield, with the experiment package inside, was hoisted to the predrop position at the top of the facility (fig. 6). The wire support was attached to the release system, and the entire assembly was suspended from the wire. After final electrical checks and switching to internal power, the system was released. After completion of the test, the experiment package and drag shield were returned to the preparation area.

REFERENCES

1. Symons, Eugene P.; Nussle, Ralph C.; and'Abdalla, Kaleel L.: Liquid Inflow to Initially Empty, Hemispherical Ended Cylinders During Weightlessness. NASA TN D-4628, 1968.
2. Symons, Eugene P.: Interface Stability During Liquid Inflow to Initially Empty Hemispherical Ended Cylinders in Weightlessness. NASA TM X-2003, 1970.
3. Symons, Eugene P.: Liquid Inflow to Partially Full, Hemispherical-Ended Cylinders During Weightlessness. NASA TM X-1934, 1969.
4. Albertson, M. L.; Dai, Y. B.; Jensen, R. A.; and Rouse, Hunter: Diffusion of Submerged Jets. Am. Soc. Civil Eng. Proc., vol. 74, no. 10, Dec. 1948, pp. 1571-1596.
5. Symons, Eugene P.; and Labus, Thomas L.: An Experimental Investigation of an Axisymmetric Fully Developed Laminar Free Jet. NASA TN D-6304, 1971.
6. Rouse, Hunter, ed.: Engineering Hydraulics. John Wiley & Sons, Inc., 1950.
7. Siegert, Clifford E.; Petrash, Donald A.; and Otto, Edward W.: Time Response of the Liquid-Vapor Interface After Entering Weightlessness. NASA TN D-2458, 1964.

TABLE I. - PROPERTIES OF TEST LIQUIDS

[Static contact angle with cast acrylic plastic in air, 0°.]

Liquids	Surface tension at 20° C, σ, N/cm (10^5 dynes/cm)	Density at 20° C, ρ, g/cm^3	Viscosity at 20° C, μ, g/(cm)(sec)	Specific surface tension, β, cm^3/sec^2
Anhydrous ethanol	22.3×10^{-5}	0.79	1.2×10^{-2}	28.3
Trichlorotrifluoroethane	18.6×10^{-5}	1.58	$.7\times10^{-2}$	11.8
Carbon tetrachloride	26.9×10^{-5}	1.59	$.97\times10^{-2}$	16.8

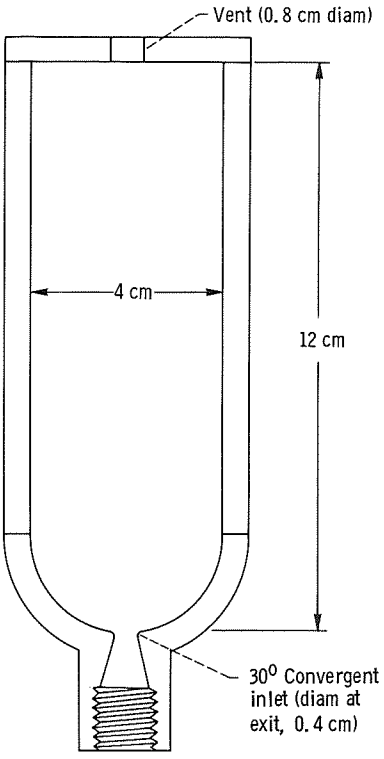

Figure 1. - Experiment tank.

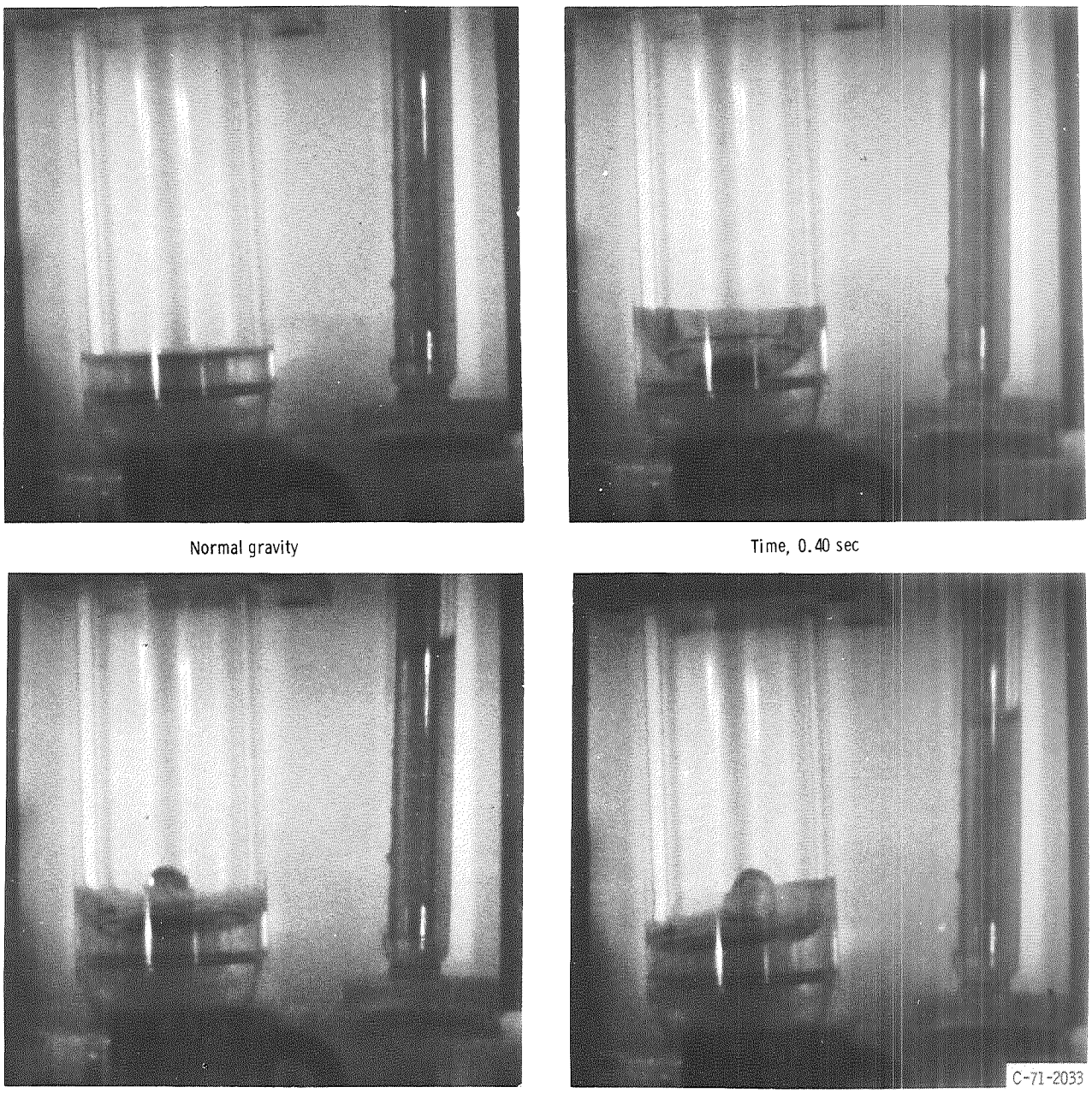

Normal gravity

Time, 0.40 sec

Time, 1.25 sec

Time, 2.09 sec

(a) Liquid, carbon tetrachloride; height of liquid above inlet, 2.4 centimeters; inflow velocity, 25.5 centimeters per second.

Figure 2. - Stable interface behavior. Tank radius, 2 centimeters; inlet line radius, 0.2 centimeter.

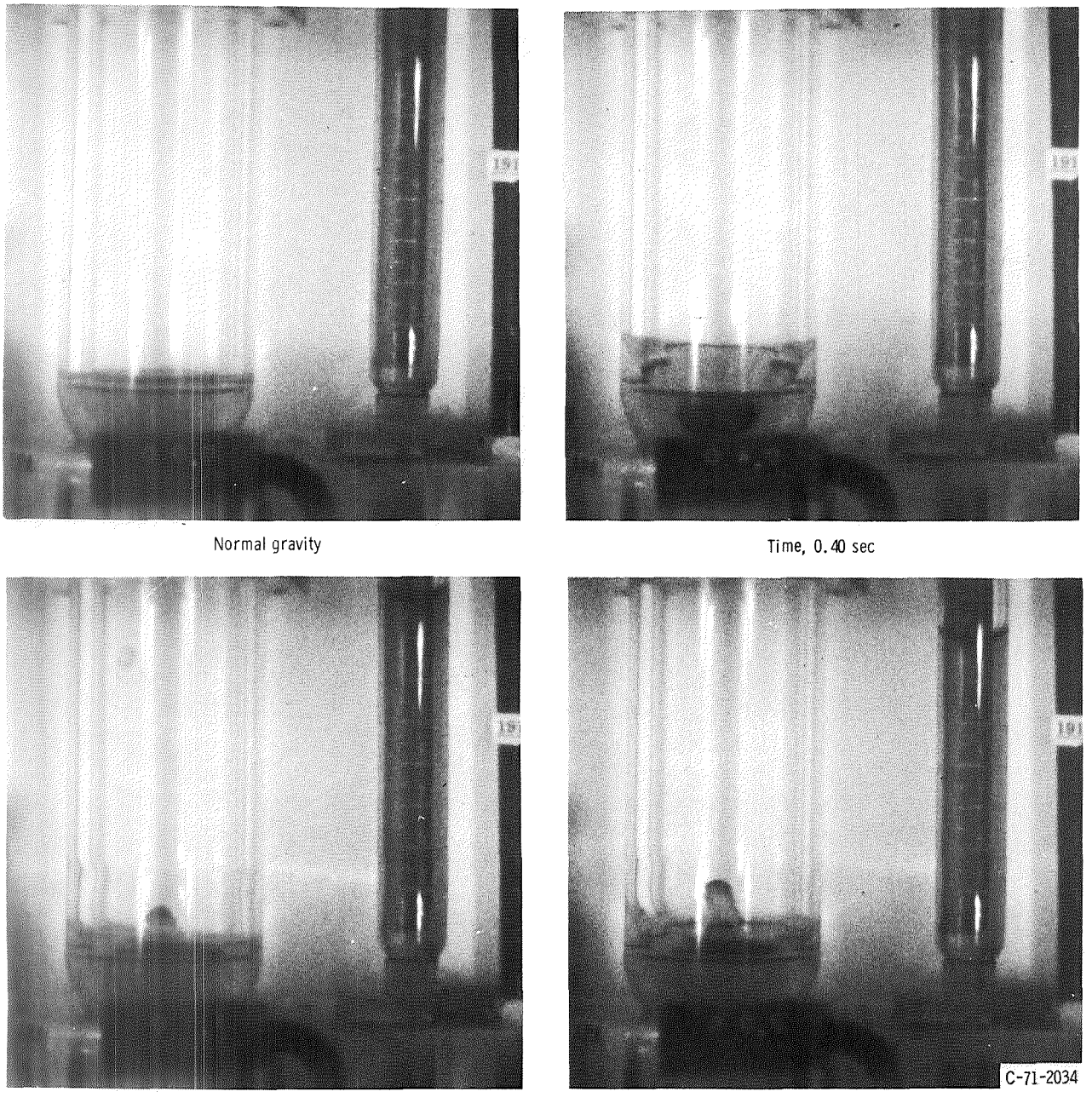

Normal gravity

Time, 0.40 sec

Time, 1.10 sec

Time, 2.05 sec

(b) Liquid, trichlorotrifluoroethane; height of liquid above inlet, 1.6 centimeters; inflow velocity, 16.1 centimeters per second.

Figure 2. - Continued.

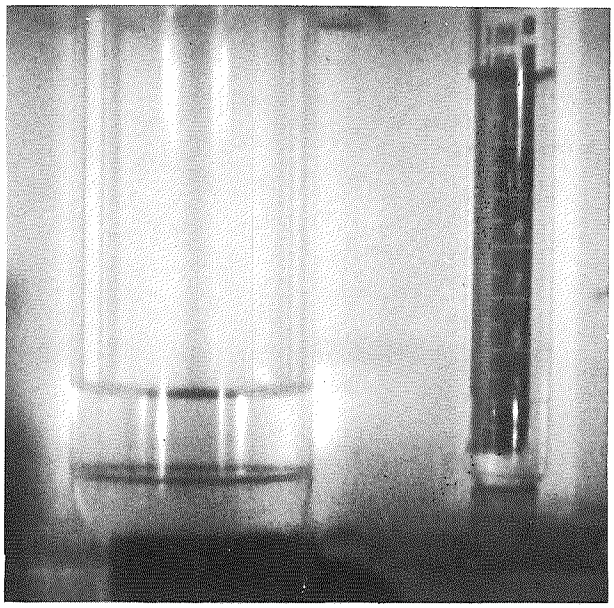

Normal gravity

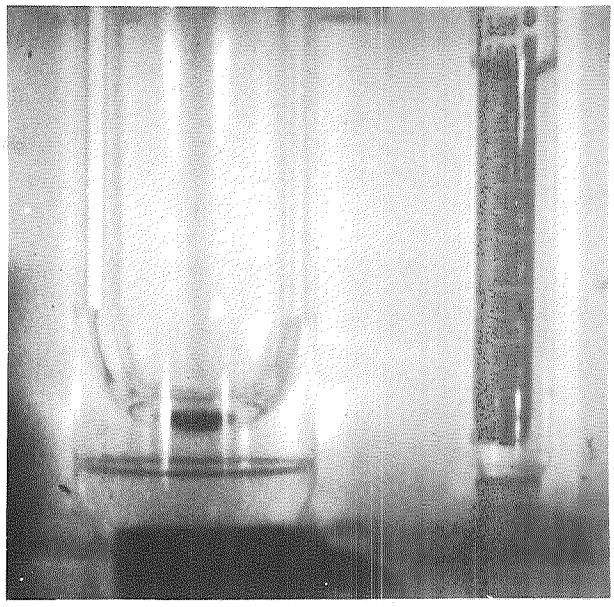

Time, 0.40 sec

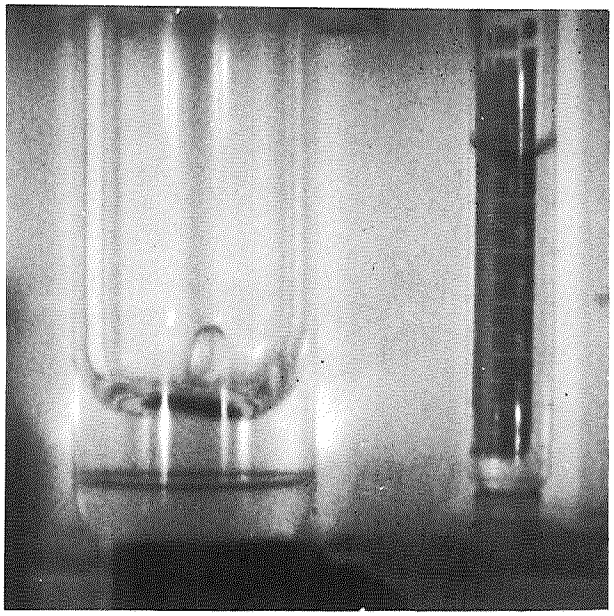

Time, 1.25 sec

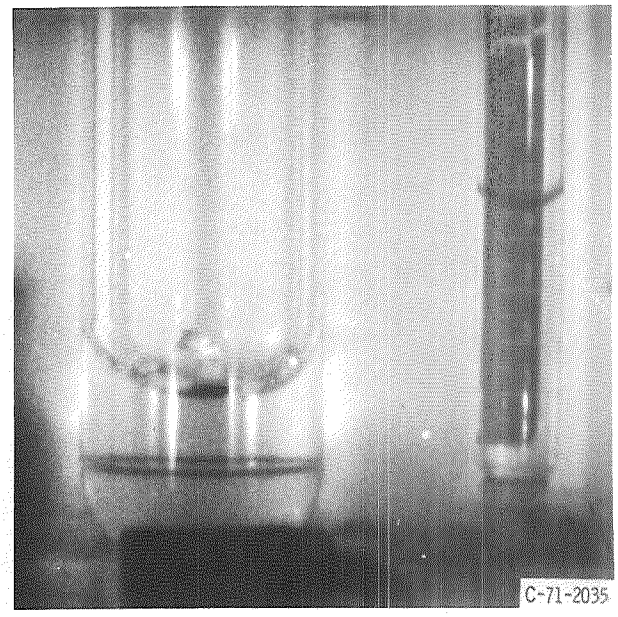

Time, 2.05 sec

(c) Liquid, ethanol; height of liquid above inlet, 3.2 centimeters; inflow velocity, 23.6 centimeters per second.

Figure 2. - Concluded.

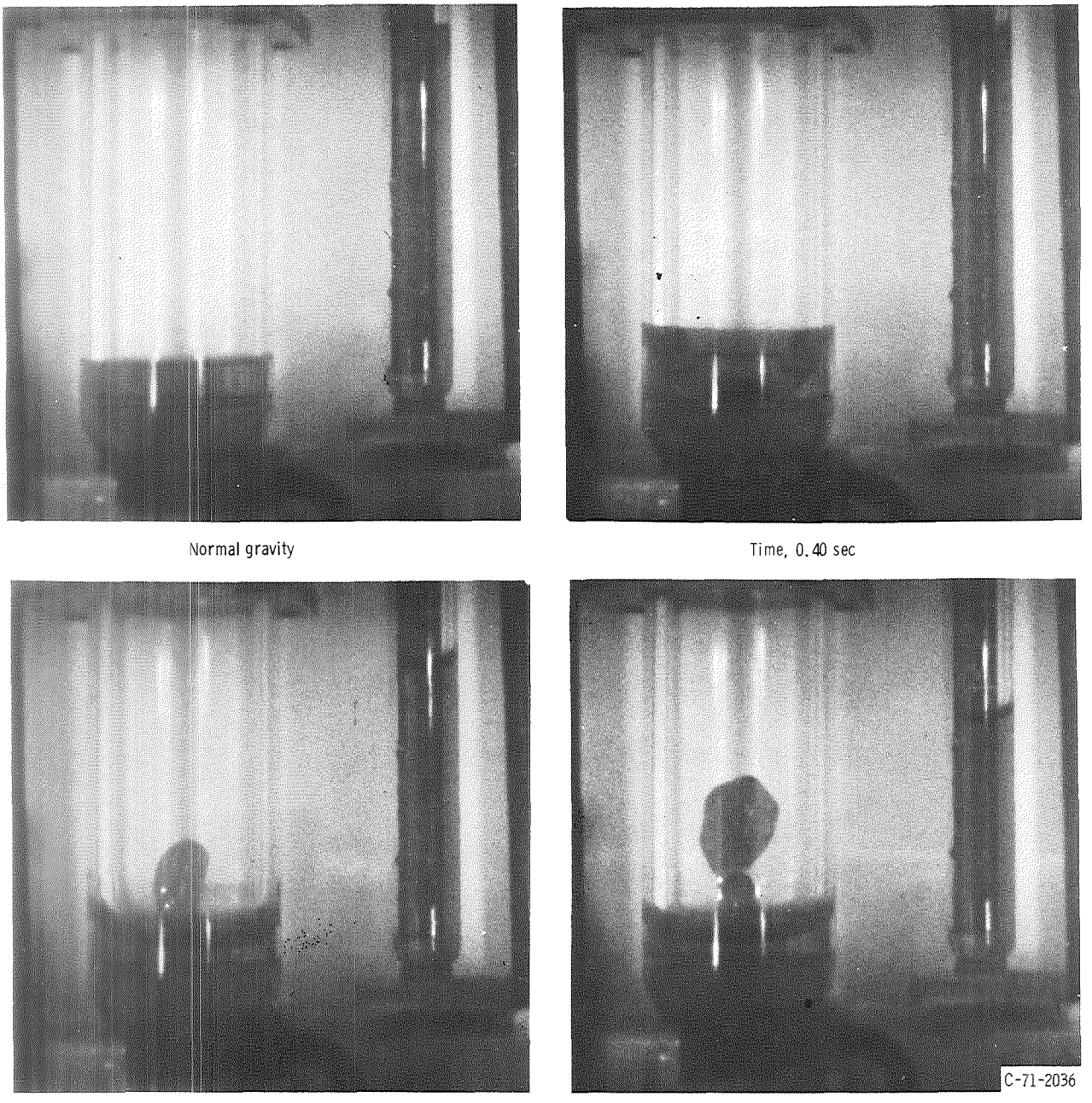

Normal gravity

Time, 0.40 sec

Time, 1.25 sec

Time, 2.09 sec

(a) Liquid, carbon tetrachloride; height of liquid above inlet, 2.4 centimeters; inflow velocity, 28.4 centimeters per second.

Figure 3. - Unstable interface behavior. Tank radius, 2 centimeters; inlet line radius, 0.2 centimeter.

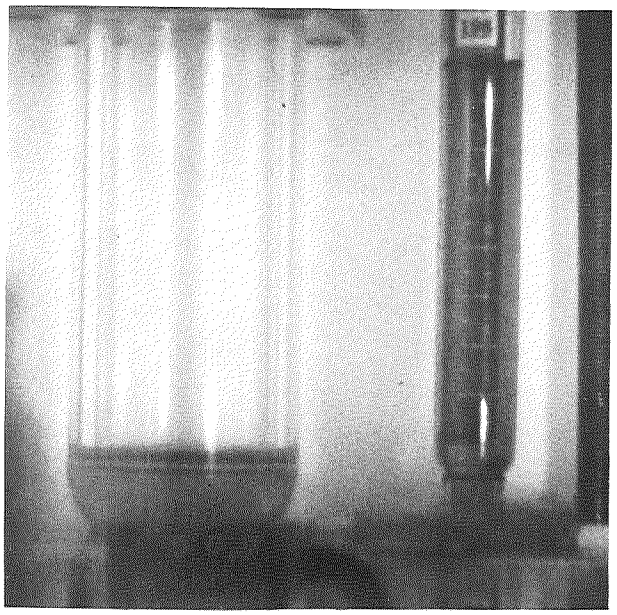

Normal gravity

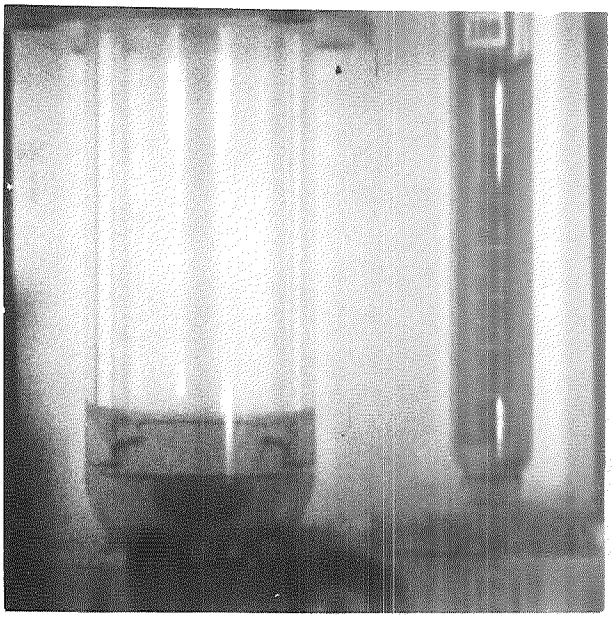

Time, 0.40 sec

Time, 1.10 sec

Time, 2.05 sec

(b) Liquid, trichlorotrifluoroethane; height of liquid above inlet, 1.6 centimeters; inflow velocity, 21.2 centimeters per second.

Figure 3. - Continued.

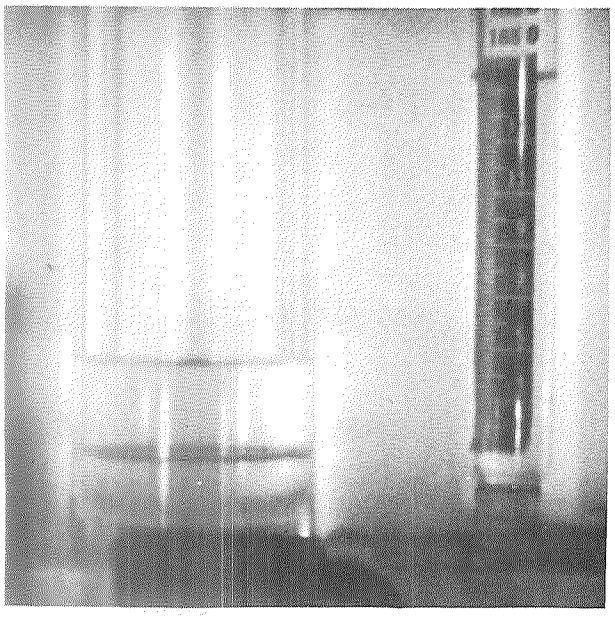

Normal gravity

Time, 0.40 sec

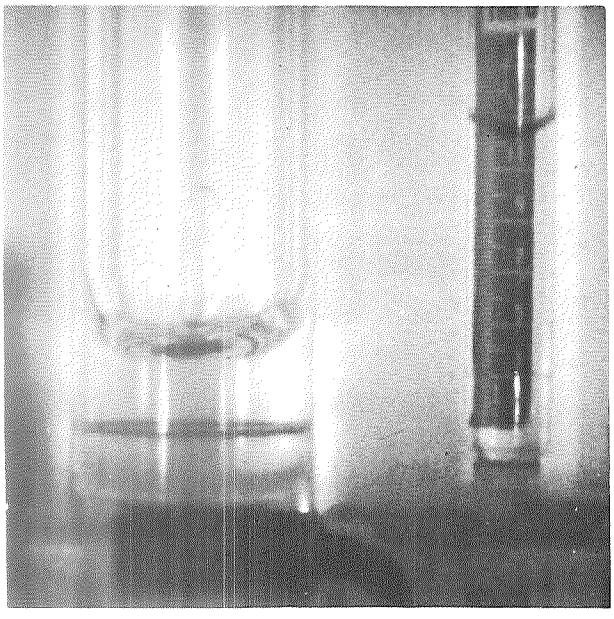

Time, 1.25 sec

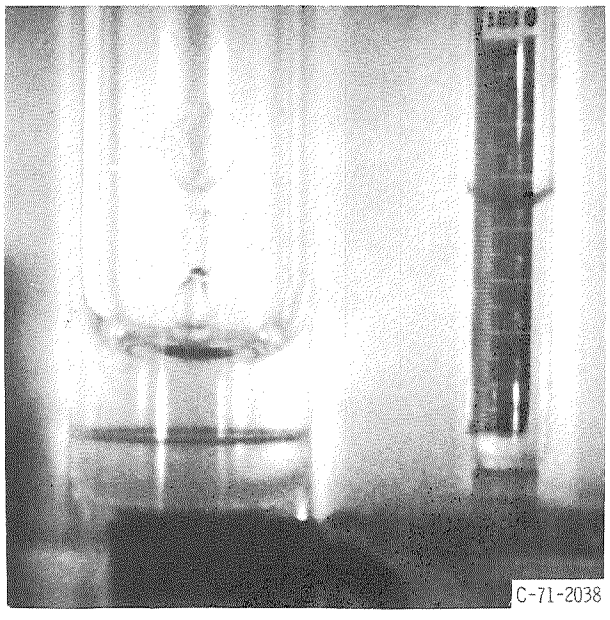

Time, 2.05 sec

(c) Liquid, ethanol; height of liquid above inlet, 3.2 centimeters; inflow velocity, 24.9 centimeter per second.

Figure 3. - Concluded.

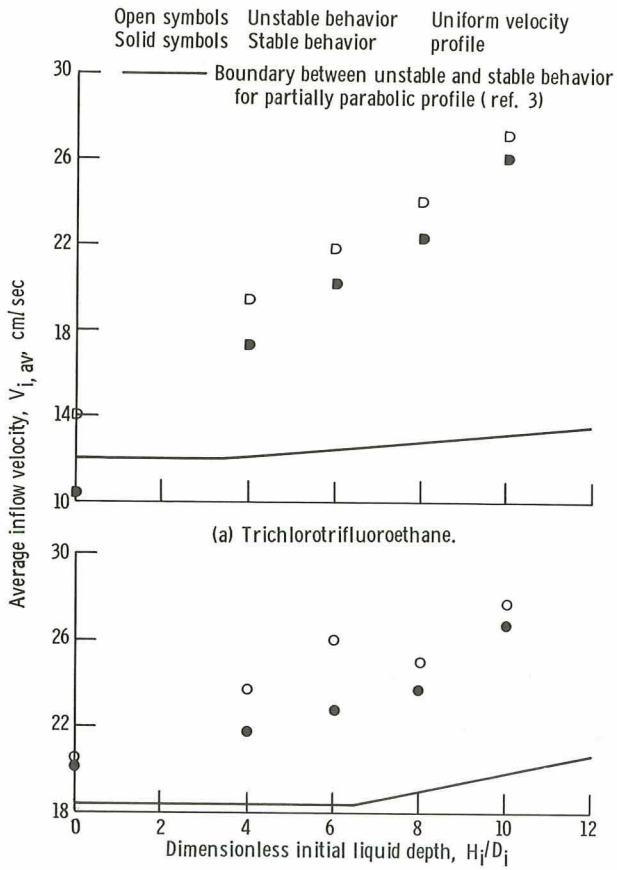

Figure 4. - Effect of initial velocity profile and initial liquid depth. on critical inflow velocity.

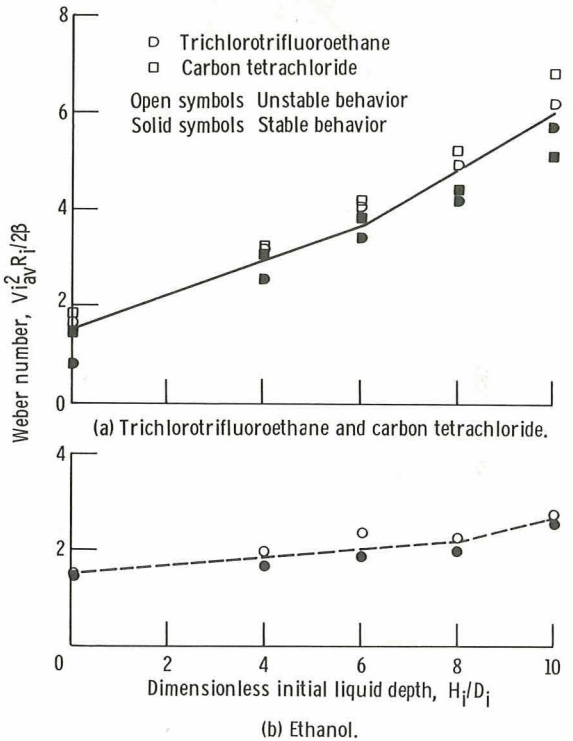

Figure 5. - Weber number as function of dimensionless initial liquid depth.

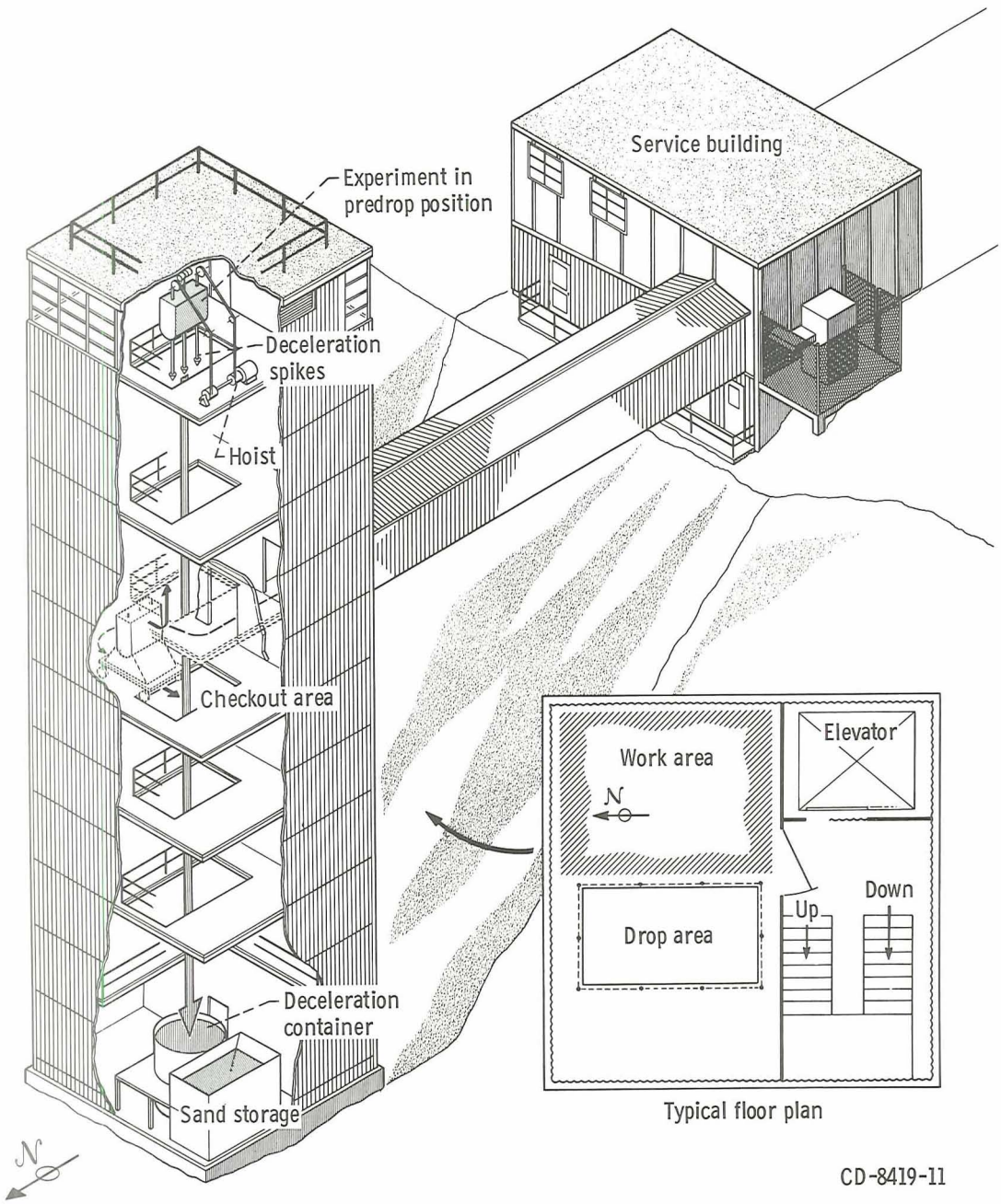

Figure 6. - 2.2-Second Zero-Gravity Facility.

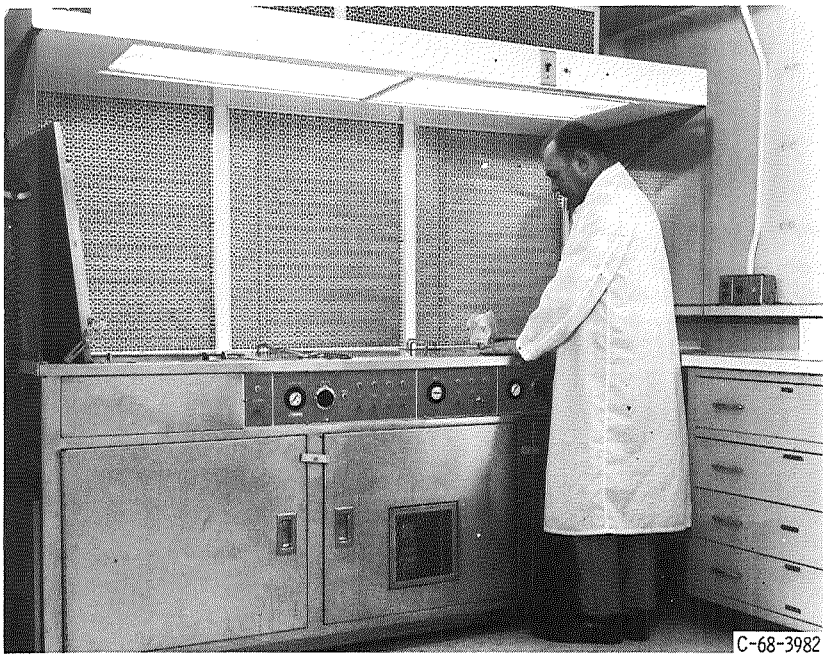

(a) Ultrasonic cleaning system.

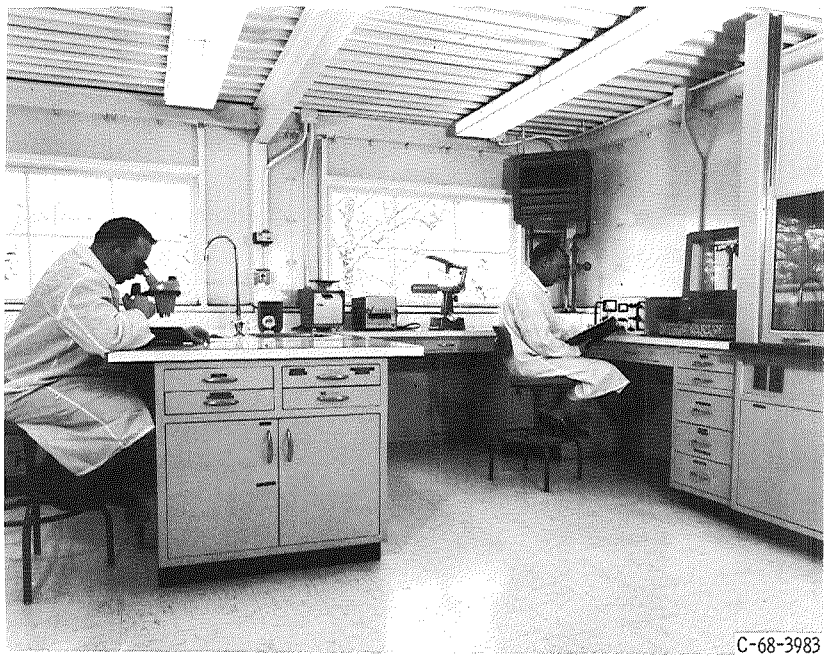

(b) Laboratory equipment.

Figure 7. - Controlled environment room.

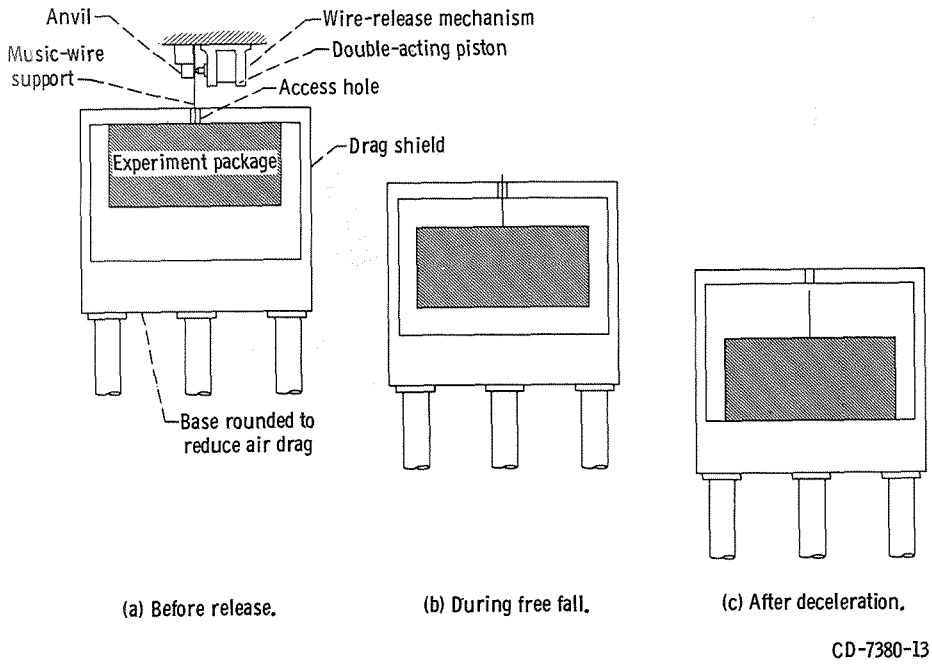

Figure 8. - Position of experiment package and drag shield before, during, and after test drop.

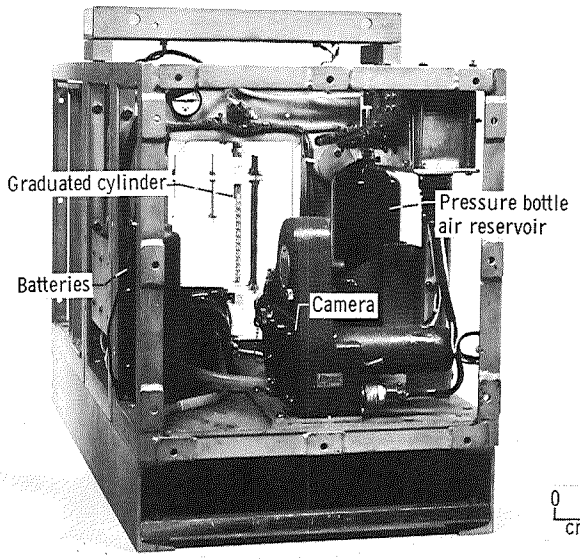

C-67-375

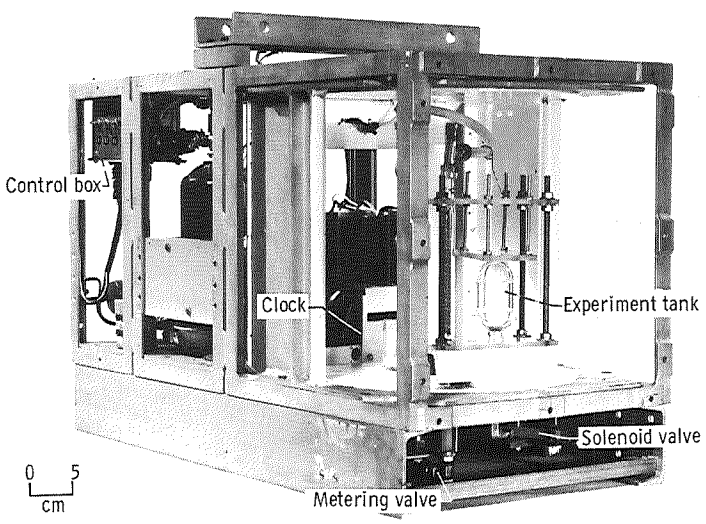

C-67-376

Figure 9. - Experiment package.

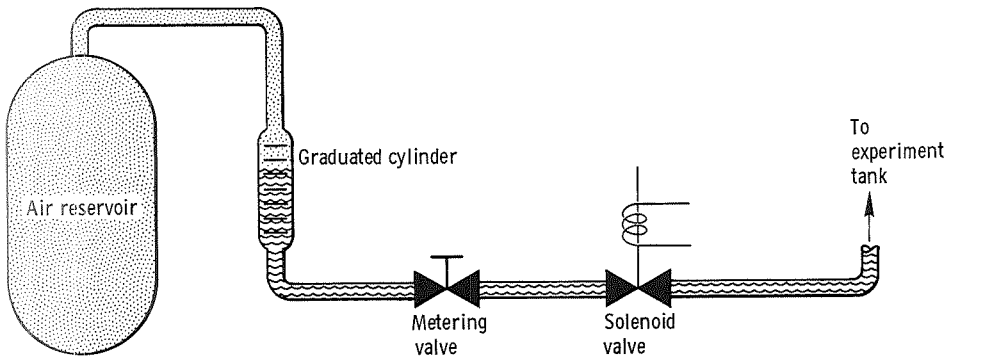

Figure 10. - Pumping system schematic.

NASA-Langley, 1971 —— 12 E-6346

NATIONAL AERONAUTICS AND SPACE ADMINISTRATION
WASHINGTON, D. C. 20546

OFFICIAL BUSINESS
PENALTY FOR PRIVATE USE $300

FIRST CLASS MAIL

POSTAGE AND FEES PAID
NATIONAL AERONAUTICS AND
SPACE ADMINISTRATION

POSTMASTER: If Undeliverable (Section 158 Postal Manual) Do Not Return

"The aeronautical and space activities of the United States shall be conducted so as to contribute . . . to the expansion of human knowledge of phenomena in the atmosphere and space. The Administration shall provide for the widest practicable and appropriate dissemination of information concerning its activities and the results thereof."

—NATIONAL AERONAUTICS AND SPACE ACT OF 1958

NASA SCIENTIFIC AND TECHNICAL PUBLICATIONS

TECHNICAL REPORTS: Scientific and technical information considered important, complete, and a lasting contribution to existing knowledge.

TECHNICAL NOTES: Information less broad in scope but nevertheless of importance as a contribution to existing knowledge.

TECHNICAL MEMORANDUMS: Information receiving limited distribution because of preliminary data, security classification, or other reasons.

CONTRACTOR REPORTS: Scientific and technical information generated under a NASA contract or grant and considered an important contribution to existing knowledge.

TECHNICAL TRANSLATIONS: Information published in a foreign language considered to merit NASA distribution in English.

SPECIAL PUBLICATIONS: Information derived from or of value to NASA activities. Publications include conference proceedings, monographs, data compilations, handbooks, sourcebooks, and special bibliographies.

TECHNOLOGY UTILIZATION PUBLICATIONS: Information on technology used by NASA that may be of particular interest in commercial and other non-aerospace applications. Publications include Tech Briefs, Technology Utilization Reports and Technology Surveys.

Details on the availability of these publications may be obtained from:

SCIENTIFIC AND TECHNICAL INFORMATION OFFICE

NATIONAL AERONAUTICS AND SPACE ADMINISTRATION

Washington, D.C. 20546